AIP Journal of Applied Physics

Anomalous thermal hysteresis of two first order phase transitions in relaxor ferroelectric 0.945 Pb(Zn1/3Nb2/3)O3-0.055PbTiO3 crystals studied by Brillouin scattering

Md. Saidul Islam, Shinya Tsukada, and Seiji Kojima

Citation: Journal of Applied Physics **119**, 094106 (2016); doi: 10.1063/1.4942858
View online: http://dx.doi.org/10.1063/1.4942858
View Table of Contents: http://scitation.aip.org/content/aip/journal/jap/119/9?ver=pdfcov
Published by the AIP Publishing

Anomalous thermal hysteresis of two first order phase transitions in relaxor ferroelectric 0.945 $Pb(Zn_{1/3}Nb_{2/3})O_3$-0.055$PbTiO_3$ crystals studied by Brillouin scattering

Md. Saidul Islam,[1,2,a)] Shinya Tsukada,[3] and Seiji Kojima[1,b)]
[1]*Graduate School of Pure and Applied Sciences, University of Tsukuba, Tsukuba, Ibaraki 305-8573, Japan*
[2]*Department of Materials Science and Engineering, University of Rajshahi, Rajshahi 6205, Bangladesh*
[3]*Faculty of Education, Shimane University, Matsue City, Shimane 690-8504, Japan*

(Received 25 October 2015; accepted 14 February 2016; published online 3 March 2016)

The thermal hysteresis has been studied by Brillouin scattering in the relaxor ferroelectric $(1-x)Pb(Zn_{1/3}Nb_{2/3})O_3$-$xPbTiO_3$ with $x = 0.055$ (i.e., below the morphotropic phase boundary composition $x \sim 0.08$). On heating from room temperature, the first order rhombohedral to tetragonal phase transition occurs at $T_{R\text{-}T} = 397$ K, then the first order tetragonal to cubic transition occurs at $T_{T\text{-}C} = 425$ K. However, on cooling from high temperature, only the diffusive phase transition was observed around $T_{C\text{-}R} = 401$ K. Such anomalous thermal hysteresis is attributed to the metastable non-equilibrium states induced by supercooling due to quenching of nano-domains by the random electric fields of the B-site charge disorder. © *2016 AIP Publishing LLC*. [http://dx.doi.org/10.1063/1.4942858]

I. INTRODUCTION

Relaxor-based perovskite ferroelectric single crystals, $(1-x)Pb(Zn_{1/3}Nb_{2/3})O_3$-$xPbTiO_3$ (PZN-100xPT) and $(1-x)Pb(Mg_{1/3}Nb_{2/3})O_3$-$xPbTiO_3$ (PMN-100xPT), exhibit extraordinarily high electromechanical properties that make them potential candidates for practical applications such as next-generation sensors, medical imaging, and broadband transducers.[1–3] Pure $Pb(Zn_{1/3}Nb_{2/3})O_3$ (PZN) undergoes a diffuse ferroelectric phase transition from cubic to rhombohedral symmetry at $T_{C\text{-}R} = 413$ K by the charge disorder of Zn^{2+} and Nb^{5+} at the B-site.[4] In PZN-100xPT system, with the increase of $PbTiO_3$ (PT) content, the cubic to rhombohedral phase transition splits into two phase transitions from cubic to tetragonal and then to rhombohedral with the PT content (x) from 0.05 to 0.12. A morphological phase boundary (MPB) appears between $x = 0.08$ and 0.12, where rhombohedral and tetragonal phases co-exist.[5–7] The MPB divides the ferroelectric phase in the PZN-100xPT phase diagram into two regions of Ti-poor rhombohedral and Ti-rich tetragonal phases. The existence of a monoclinic ferroelectric phase was reported near the MPB in a narrow compositional range at temperatures below room temperature.[8] However, the superior piezoelectric response of PZN-100xPT has been associated with the MPB, and these are attributed to the intermediate monoclinic phases that allow the polarization rotation in the symmetry plane. On further cooling, a monoclinic (Cm)-monoclinic (Cc) transition occurs to an octahedrally tilted phase.[9,10] Moreover, an additional cell-doubling phase transition below room temperature due to antiphase tilts of oxygen octahedra was found in the MPB compositions by electric measurements.[11] The above scenario implies that the symmetry and the phase transitions of PZN-100xPT near MPB were more complicated than those of previous reports, and monoclinic and/or orthorhombic symmetries appear with and/or without biasing electric field depending on the composition.[12,13] However, the exact crystal symmetry, the elastic properties, and the dynamical features of phase transitions remain still unclear not only near MPB region but also over the whole composition in a wide temperature range, which provoke a strong controversy and investigation.[14–17]

In $Pb(B_{1/3}B'_{2/3})O_3$ based relaxors, the charge disorder of $(B)^{2+}$ and $(B')^{5+}$ at the B-site gives rise to random fields (RFs), which is considered to be the origin of the relaxor behavior characterized by their strong frequency dispersion of dielectric constant. The local charge fluctuations provoke the ferroelectric symmetry breaking on a nanometer scale called polar nanoregions (PNRs) at high temperatures.[4,18] While there is another stable nanosize local order, namely, chemically ordered regions (CORs) correspond to regions of regularly ordered $(B)^{2+}(B')^{5+}$ pairs at the doubled chemical unit size level. The CORs carry negative charges, $\{[(A)^{2+}(B)^{2+}(O)^{6-}]\}^{2-} + \{[(A)^{2+}(B')^{5+}(O)^{6--}]\}^{1+} = \{2[(A)^{2+}(B)^{4+} + (O)^{6-}]\}^{1-}$, and are intense sources of quenched RFs. It is suggested that the CORs have an influence on the diffuseness of a ferroelectric transition.[19] The CORs are temperature independent, while the PNRs show the remarkable temperature dependence and play the essential role in the nature of relaxors.

The evolution of PNRs is related to four characteristics temperatures, upon cooling, (i) the Burns temperature, T_B, at which dynamic PNRs appear due to the short-lived correlation between the off-centered ions; (ii) the intermediate temperature, T^*, below which the dynamic PNRs transfer to static ones with a rapid growth in size owing to the long-lived correlation between the atomic displacements of off-centered ions;[20] (iii) the temperature at the dielectric peak of the lowest frequency, T_m; and (iv) the ferroelectric phase-transition temperature, T_C.[21]

A lot of experimental efforts have been made by neutron, x-ray, inelastic light scattering, electron diffraction, etc., to unveil the structural and dynamical features of PNRs,

a)sayeed_mse@ru.ac.bd
b)kojima@bk.tsukuba.ac.jp

however, it remains in controversy, especially over a paraelectric phase with high symmetry.[6,22] A recent report on the acoustic emission (AE) of Pb-based relaxors at $T^* \sim 500$ K suggests that the martensitic transformation of PNRs generates AE bursts that were detectable by the piezoelectric sensor in the kilohertz range.[23] However, the Brillouin scattering technique probes acoustic modes and a central peak (CP) in the gigahertz range with a wavelength much shorter than that of the standard ultrasonic experiment. Therefore, the Brillouin light scattering measurements on PZN-100xPT can give us new insights into the dynamics of a phase transition, including the local polarization fluctuations of PNRs in the frequency range from 1 to 1000 GHz.[24]

Up to the present, the Brillouin scattering studies have been performed on PZN[25,26] and the PZN-xPT solid solutions, i.e., PZN-4.2PT,[14] PZN-4.5PT,[14,27] PZN-7PT,[20,28,29] PZN-9PT,[30–32] PZN-15PT,[33] and PZN-20PT.[34] From the previous study, it is commonly agreed that the dynamical feature of a phase transition is strongly dependent on PT content, i.e., the PT content lower than $x = 0.09$ exhibits a relaxor behavior with a diffuse and dispersive permittivity maximum and transforms the relaxor state into a stable ferroelectric phase with rhombohedral symmetry upon cooling. In contrast, PZN-15PT and PZN-20PT undergo a first-order ferroelectric phase transition from the paraelectric cubic phase to the tetragonal ferroelectric phase at $T_{C\text{-}T}$ without any diffusive nature and do not undergo into any rhombohedral ferroelectric phase upon further cooling.[30,32] It is reported that a first-order phase transition for PZN-4.42PT, while the phase transition sequence changes to second-order for PZN-4.5PT. In addition, a huge thermal hysteresis was observed in PZN-7PT but a small or no thermal hysteresis was observed in PZN-4.42PT and PZN-4.5PT.[14,20] All these facts indicate that the physical and dynamical features of phase transitions were very sensitive to the PT content.[14] Therefore, the detailed survey for every nominal composition is very crucial to enrich the knowledge about PZN-100xPT. In the present work, we report the detailed temperature dependent micro-Brillouin study of 0.945Pb $(Zn_{1/3}Nb_{2/3})O_3$-0.055$PbTiO_3$ (PZN-5.5PT) crystals.

II. EXPERIMENTAL

The flux grown PZN-5.5PT single crystals were purchased from Microfine Materials Technologies co. Ltd. A micro-Brillouin scattering system with a $(3+3)$ pass Sandercock-type tandem Fabry-Perot interferometer (FPI) was used to measure the Brillouin spectra of PZN-5.5PT single crystals at a backward scattering geometry without a polarizer (vertical to open, VO). Acoustic phonons and a central peak were measured with free spectral ranges (FSR) of 75 and 300 GHz, respectively. An optical microscope (OLYMPUS, BX 41) was combined with the FPI to achieve a focal point of 10 μm. A single-frequency green YAG laser with a wavelength of 532 nm was used to excite a sample with a power of 50 mW. A conventional photon counting system and a multi-channel analyzer were used to detect and average the signals. The temperature of a sample was controlled by a heating/cooling stage (Linkam, THMS600) from 350 K to 830 K with ± 0.1 K accuracy.

III. RESULTS AND DISCUSSION

A. Elastic anomaly

Figure 1 shows the Brillouin scattering spectra of a PZN-5.5PT crystal upon heating and cooling at selected temperatures with FSR of 75 GHz. The spectrum contains a longitudinal acoustic (LA) mode around ± 41 GHz, a transverse acoustic (TA) mode around ± 24 GHz, and a CP at 0 GHz. The measured Brillouin doublets as shown in Fig. 1 were fitted by using a Lorentzian function convoluted by Gaussian instrumental function to obtain the Brillouin frequency shift (ν_{LA}) and the full-width at half maximum (FWHM or Γ_B). The temperature dependences of ν_{LA} and FWHM of LA mode are shown in Fig. 2. The elastic anomalies of successive phase transitions were clearly observed at 397 K ($T_{R\text{-}T}$) and at 425 K ($T_{T\text{-}C}$) upon heating, corresponding to a rhombohedral to tetragonal and to a tetragonal to cubic phase transition, respectively. The observed $T_{R\text{-}T}$ and $T_{T\text{-}C}$ are in good agreement with those of the reported phase diagram.[7] These transition anomalies are attributed to a strong coupling between strain fluctuation and

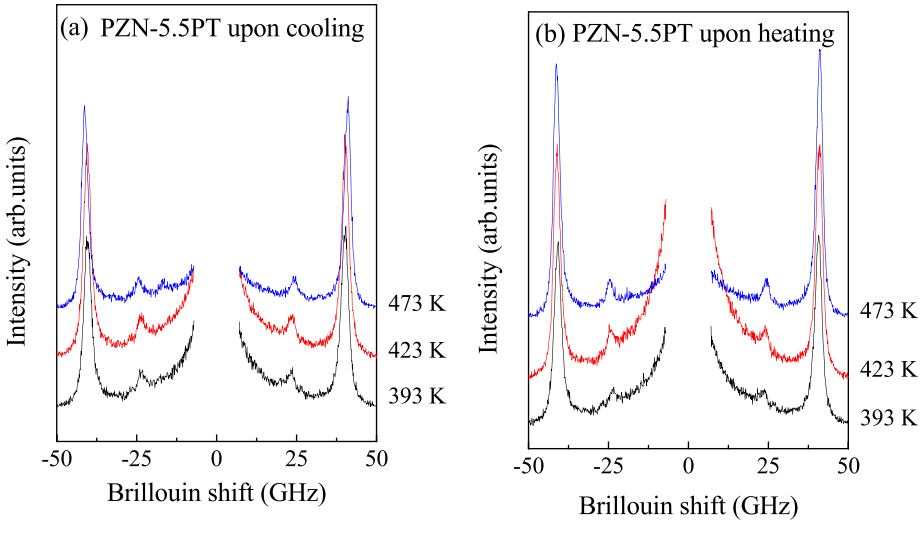

FIG. 1. Brillouin scattering spectra of a PZN-5.5PT single crystal at selected temperatures in (a) upon cooling and (b) upon heating cycle.

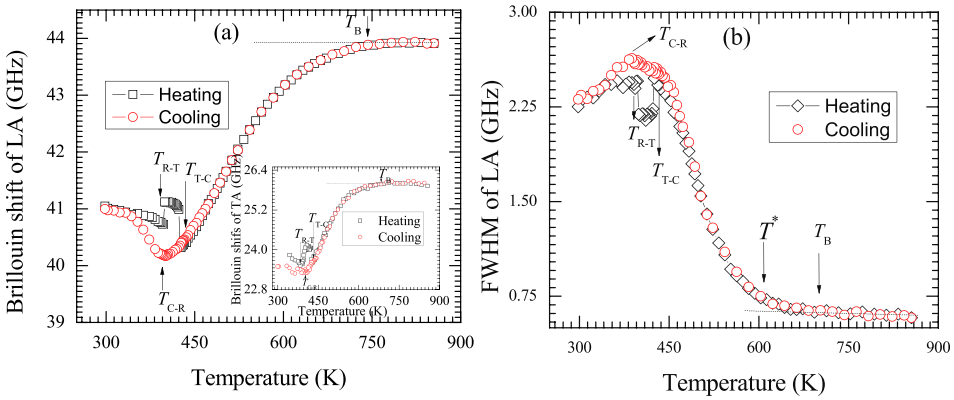

FIG. 2. Temperature dependence of (a) the Brillouin shift [inset of the TA mode] and (b) the FWHM of the LA mode of a PZN-5.5PT single crystal.

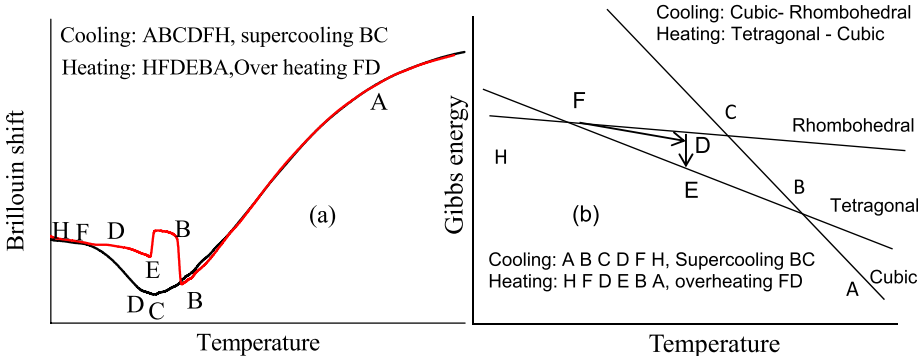

FIG. 3. (a) Thermal hysteresis in ν_B and (b) schematic of free energies predicted for PZN–5.5PT around the phase transition temperatures to explain the observed thermal hysteresis.

polarization fluctuation. In contrast, upon cooling from the high temperature in a cubic phase, a diffuse transition anomaly was observed around 401 K ($T_{C\text{-}R}$) corresponding to a cubic to tetragonal phase transition. The temperature dependent ν_{TA} of TA mode is shown in the inset of Fig. 2(a), which also shows successive phase transition anomalies around 397 K ($T_{R\text{-}T}$) and at 425 K ($T_{T\text{-}C}$) upon heating, while a diffuse transition anomaly around 401 K ($T_{C\text{-}R}$) upon cooling. The FWHM of a TA mode could not be determined with good accuracy.

The step-like increases of ν_{LA} at $T_{R\text{-}T}$ and $T_{T\text{-}C}$ and the existence of thermal hysteresis indicate the first order nature of two phase transitions. It is known that for a first order phase transition, more than one minimum should be concerned in an energy landscape, while in the present case, at least three phases—cubic, tetragonal, and rhombohedral—should be taken into account. These three phases have similar free energies around the phase transitions; as a result, the nonequilibrium states can be easily achieved through supercooling, leading to the appearance of the large thermal hysteresis. A schematic figure shown in Fig. 3, when the sample in a cubic phase is cooled from high temperature (A), a supercooled state starts to appear at 425 K (B) and it continues down to $T_{C\text{-}R} \sim 401$ K along the line BC and finally it undergoes a cubic (metastable) to rhombohedral (metastable) phase transition at C under the nonequilibrium condition. The supercooled metastable rhombohedral state becomes stable below F (333 K). However, during heating from a low temperature (H), the nucleation of tetragonal embryos in a rhombohedral matrix starts to appear at F (333 K). The nucleation percolates at D (397 K), and eventually the rhombohedral phase changes into the stable tetragonal phase. Finally, the tetragonal phase transforms into a stable cubic phase at $T_{T\text{-}C}$ (B).

A similar successive phase transition phenomenon with a huge thermal hysteresis was also observed for PZN-7PT,[21] while a tiny thermal hysteresis was reported for PZN-4.2PT.[14]

B. CP and relaxation time

The temperature dependence of the CP of a PZN-5.5PT crystal was measured using FSR of 300 GHz upon cooling. Figure 4 shows the semi-log plot of broadband Brillouin scattering spectra at selected temperatures. It is evident that the CP is almost absent at the highest temperature of 473 K and grows substantially upon cooling down to $T_{C\text{-}R}$. Under

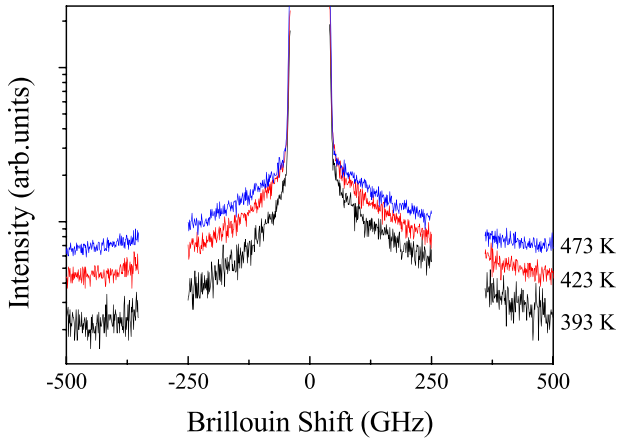

FIG. 4. Brillouin scattering spectra of a PZN-5.5PT single crystal at selected temperatures in wide frequency ranges for the observation of the CP.

the assumption of a single relaxation process, the CP was fitted by using a single Lorentzian function centered at zero frequency shift, and the relaxation time τ_{CP} is calculated by the equation, $\pi \times$ (FWHM of CP) $\times \tau_{CP} = 1$. The temperature dependence of the inverse τ_{CP} is plotted, as shown in Fig. 5. Upon cooling from the high temperature, the smeared slowing-down maximizes at temperature close to $T_{C\text{-}R}$. Such a stretching-type behavior of the relaxation time under the influence of random fields is described by the extended Curie-Weiss law following empirical relation:[35,36]

$$\frac{1}{\tau} = \frac{1}{\tau_0} + \frac{1}{\tau_1}\left(\frac{T - T_C}{T_C}\right)^{\beta}, \quad \beta \geq 1, \text{for } T > T_{C-R}, \qquad (1)$$

where β is the stretch index. In the case of $\beta = 1.0$, Eq. (1) gives the normal critical slowing down without random fields. In the case of $\beta > 1.0$, the slowing down of relaxation time is suppressed and/or stretched by the increase of the strength of random fields. As shown Fig. 5, it is found that the value of $\beta = 1.99$ yields a reasonable reproduction. $\tau_0 = 0.39$ ps and $T_C = 367$ K. The value of τ_0 is much smaller (14 ps) than that of $0.70Pb(Sc_{1/2}Nb_{1/2})O_3$-$0.30PbTiO_3$ (PSN-30PT), reflecting the first-order nature of the ferroelectric phase transition in PZN-5.5PT.[24]

The critical slowing down is a characteristic of an order-disorder phase transition which was observed in PZN-15PT. In PZN-7PT, the slowing down was observed, however, the critical slowing down was suppressed near T_C due to the existence of CORs by the strong random fields.[25,35] Similar phenomena were reported in PMN-100xPT.[37] In PMN-100xPT, a strong spatial correlation between PNRs and CORs was suggested by first principle calculations.[38] However, in PMN-100xPT, the size of CORs decreases with the increase of Ti-content and CORs finally disappear at $x \sim 0.4$, as revealed by the transmission electron microscopy[39] and the synchrotron X-ray scattering studies.[40] Therefore, in PMN-55PT with weak random fields, the critical slowing down was clearly observed by Brillouin scattering.[37] The dynamic behavior observed in PZN-100xPT can be explained in a similar way. In PZN-100xPT of the low PT content, such as PZN-7PT, both the PNRs and the CORs could coherently contribute to the phase transition dynamics, and the critical slowing down is suppressed due to the existence of CORs. Therefore, the observed stretched like slowing down can be caused by the strong interaction between the PNRs and the CORs.

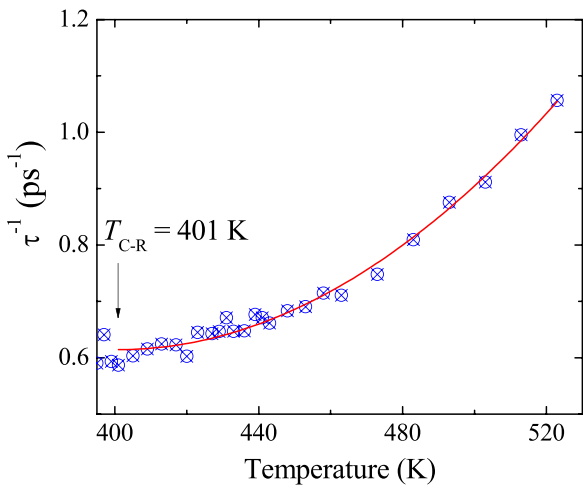

FIG. 5. Temperature dependence of the inverse relaxation time of a PZN-5.5PT single crystal.

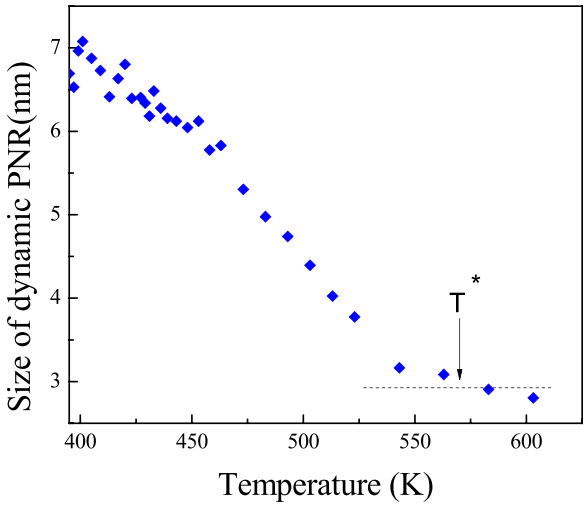

FIG. 6. Temperature dependence of the size of dynamic PNRs of a PZN-5.5PT single crystal.

C. Size of dynamic PNR

The temperature evolution of the dynamic PNRs is also important in understanding the dynamics of PNRs in relaxor ferroelectrics. According to the neutron diffuse scattering study for PZN, a diffuse scattering intensity peak appears at $T_B \sim 720$ K, and the formation of static PNRs starts below temperature $T^* \sim 450$ K,[41] and similarly, $T^* \sim 500$ K for PZN-4.5PT, and $T^* \sim 550$ K for PZN-9PT.[42] For PZN-4.5PT, $T_B \sim 800$ K and $T^* \sim 550$ K were reported by Raman scattering study.[43] For PZN-4.5PT, the correlation lengths determined from the width of diffuse scattering are about 4–18 Å at $T_B \sim 720$ K, 13–30 Å at $T^* \sim 500$ K, and 51–91 Å at 300 K, respectively.[42]

In the present Brillouin scattering study, the size of a dynamic PNR, l_{PNR}, is estimated from the relaxation time related to local polarization flipping therein and the phase velocity of the LA mode, because the characteristic length of polarization flipping can be given by the propagation length of local strain in the period of a relaxation time.[24,35] Figure 6 shows the temperature dependence of l_{PNR} for PZN-5.5PT between 400 K and 600 K. At high temperatures, the size of dynamic PNRs was about 3 nm and remains nearly constant, while near $T_{C\text{-}T}$ it starts to increase sharply and reaches 7 nm upon cooling. These values are comparable with those of PZN-4.5PT determined by the neutron diffuse scattering and the initial size of dynamic PNRs of ~2.5 nm in PZN-7PT at T^* determined by Brillouin scattering.[24]

IV. CONCLUSION

The thermal hysteresis of acoustic properties of a relaxor ferroelectric PZN-5.5PT single crystal has been studied

using Brillouin scattering. The composition of PZN-5.5PT is below the MPB at $x \sim 0.08$, and the relaxor nature is enhanced by the increase of the random fields originating from the B-site charge disorder. On heating from an equilibrium rhombohedral phase at the room temperature, the LA Brillouin shift shows the discontinuous change at the rhombohedral to tetragonal phase transition temperature, $T_{R\text{-}T} = 397$ K. For further heating, another discontinuous change was observed at the tetragonal to cubic transition temperature, $T_{T\text{-}C} = 425$ K. In contrast to the two discontinuous changes upon heating, upon cooling from a cubic phase at the high temperature, only the diffusive and continuous change of the shift was observed around $T_{C\text{-}R} \sim 401$ K. Such a remarkable thermal hysteresis can be attributed to the non-equilibrium states caused by supercooling due to blocking of the growth from nano- to macro-domains by the random fields of the B-site charge disorder.

ACKNOWLEDGMENTS

One of the authors (M. S. Islam) is thankful to the Institute of Materials Science, University of Tsukuba, for accepting as a short-term visiting research fellow. The work was partly supported by the Murata Science Foundation, Japan and the Grant-in-Aid for Young Scientists (B) program (JSPS KAKENHI Grant No. 26790040) from MEXT, Japan.

[1]R. Blinc, *Advanced Ferroelectricity, International Series of Monographs in Solid State Physics* (Oxford University Press, 2011), Vol. 151, p. 279.
[2]P.-E. Janolin, B. Dkhil, M. Davis, D. Damjanovic, and N. Setter, Appl. Phys. Lett. **90**, 152907 (2007).
[3]A. A. Bokov and Z.-G. Ye, J. Mater. Sci. **41**, 31 (2006).
[4]J. Kuwata, K. Uchino, and S. Nomura, Ferroelectrics **22**, 863 (1978).
[5]D. E. Cox, B. Noheda, G. Shirane, Y. Uesu, K. Fujishiro, and Y. Yamada, Appl. Phys. Lett. **79**, 400 (2001).
[6]Z. Kutnjak, J. Petzelt, and R. Blinc, Nature **441**, 956 (2006).
[7]J. J. Lima-Silva, I. Guedes, J. M. Filho, A. P. Ayala, M. H. Lente, J. A. Eiras, and D. Garcia, Solid State Commun. **131**, 111 (2004).
[8]B. Noheda, J. A. Gonzalo, L. E. Cross, R. Guo, S.-E. Park, D. E. Cox, and G. Shirane, Phys. Rev. B **61**, 8687 (2000).
[9]D. I. Woodward, J. Knudsen, and I. M. Reaney, Phys. Rev. B **72**, 104110 (2005).
[10]D. M. Hatch, H. T. Stokes, R. Ranjan, Ragini, S. K. Mishra, D. Pandey, and B. J. Kennedy, Phys. Rev. B **65**, 212101 (2002).
[11]Ragini, S. K. Mishra, D. Pandey, H. Lemmens, and G. Van Tendeloo, Phys. Rev. B **64**, 054101 (2001).
[12]G. Xu, H. Hiraka, G. Shirane, and K. Ohwada, Appl. Phys. Lett. **84**, 3975 (2004).
[13]G. Xu, D. Viehland, J. F. Li, P. M. Gehring, and G. Shirane, Phys. Rev. B **68**, 212410 (2003).
[14]T. H. Kim, J.-H. Ko, S. Kojima, A. A. Bokov, X. Long, and Z.-G. Ye, Appl. Phys. Lett. **100**, 082903 (2012).
[15]J. J. Zhu, W. W. Li, G. S. Xu, K. Jiang, Z. G. Hu, M. Zhu, and J. H. Chu, J. Appl. Phys. **98**, 091913 (2011).
[16]D. Phelan, X. Long, Y. Xie, Z.-G. Ye, A. M. Glazer, H. Yokota, P. A. Thomas, and P. M. Gehring, Phys. Rev. Lett. **105**, 207601 (2010).
[17]E. Buixaderas, D. Nuzhnyy, J. Petzelt, L. Jin, and D. Damjanovic, Phys. Rev. B **84**, 184302 (2011).
[18]V. Westphal, W. Kleemann, and M. D. Glinchuck, Phys. Rev. Lett. **68**, 847 (1992).
[19]W. Kleemann, J. Mater. Sci. **41**, 129 (2006).
[20]G. Burns and F. H. Dacol, Phys. Rev. B **28**, 2527 (1983).
[21]S. Tsukada, T. H. Kim, and S. Kojima, APL Mater. **1**, 032114 (2013).
[22]H. X. Fu and R. E. Cohen, Nature **403**, 281 (2000).
[23]A. A. Bokov, B. J. Rodriguez, X. Zhao, J.-H. Ko, S. Jesse, X. Long, W. Qu, T. H. Kim, J. D. Budai, A. N. Morozovska, S. Kojima, X. Tan, S. V. Kalinin, and Z.-G. Ye, Z. Kristallogr. **226**, 99 (2011).
[24]S. Kojima, S. Tsukada, Y. Hidaka, A. A. Bokov, and Z.-G. Ye, J. Appl. Phys. **109**, 084114 (2011).
[25]M. H. Kuok, S. C. Ng, H. J. Fan, M. Iwata, and Y. Ishibashi, Appl. Phys. Lett. **78**, 1727 (2001).
[26]Y. Gorouya, Y. Tsujimi, M. Iwata, and T. Yagi, Appl. Phys. Lett. **83**, 1358 (2003).
[27]D. H. Kim, J.-H. Ko, C. D. Feng, and S. Kojima, J. Appl. Phys. **98**, 044106 (2005).
[28]D. H. Kim, S. Kojima, and J.-H. Ko, Curr. Appl. Phys. **11**, 61 (2011).
[29]S. Tsukada and S. Kojima, Phys. Rev. B **78**, 144106 (2008).
[30]D. H. Kim, S. Kojima, and J.-H. Ko, J. Korean Phys. Soc. **46**(1), 131 (2005).
[31]D. H. Kim, J.-H. Ko, C. D. Feng, and S. Kojima, Appl. Phys. Lett. **87**, 072908 (2005).
[32]J.-H. Ko, D. H. Kim, and S. Kojima, Appl. Phys. Lett. **83**, 2037 (2003).
[33]M. S. Islam, S. Tsukada, W. Chen, Z.-G. Ye, and S. Kojima, J. Appl. Phys. **112**, 114106 (2012).
[34]M. H. Kuok, S. C. Ng, H. J. Fan, M. Iwata, and Y. Ishibashi, Solid State Commun. **118**, 169 (2001).
[35]S. Kojima and S. Tsukada, Ferroelectrics **405**, 32 (2010).
[36]G. Shabbir and S. Kojima, EPL **105**, 57001 (2014).
[37]J.-H. Ko, S. Kojima, A. A. Bokov, and Z.-G. Ye, Appl. Phys. Lett. **91**, 252909 (2007).
[38]S. Tinte, B. P. Burton, E. Cockayne, and U. V. Waghmare, Phys. Rev. Lett. **97**, 137601 (2006).
[39]A. D. Hilton, D. J. Barber, C. A. Randall, and T. R. Shrout, J. Mater. Sci. **25**, 3461 (1990).
[40]A. Tkachuk, P. Zschack, E. Colla, and H. Chen, *Fundamental Physics of Ferroelectrics* (American Institute of Physics, New York, 2001), Vol. 582, p. 45.
[41]D. La-Orauttapong, J. Toulouse, J. L. Robertson, and Z.-G. Ye, Phys. Rev. B **64**, 212101 (2001).
[42]D. La-Orauttapong, J. Toulouse, Z.-G. Ye, W. Chen, R. Erwin, and J. L. Roberston, Phys. Rev. B **67**, 134110 (2003).
[43]O. Svitelskiy, D. La-Orauttapong, J. Toulouse, W. Chen, and Z.-G. Ye, Phys. Rev. B **72**, 172106 (2005).